

Dipole formation by tidal flow in a channel.

M.G. Wells^{1,2} & G.J.F. van Heijst¹

1: *Dept. Applied Physics, Eindhoven University of Technology,
P.O. Box 513, NL-5600 MB Eindhoven, The Netherlands*

2: *Now at: Dept. Geology and Geophysics, Yale University
P.O. Box 208109, New Haven, CT 06520-8109, USA*

We discuss a laboratory model of dipole formation due to tidal flow through a channel connecting a bay to the sea. Tidal changes in water elevation lead to periodic flow in and out of the bay through the narrow channel. Due to flow separation there is an asymmetry between the flow entering and leaving the channel on different phases of the tide. A consequence of this asymmetry is that every tidal cycle a fraction of fluid is not returned through the channel, so that a passive tracer in the bay is successively flushed away. We consider what happens when the creation of vorticity in the channel leads to the formation of a dipole that can propagate away from the returning flow of the later phase of the tide. When the dimensionless ratio of maximum channel velocity U , width of channel w and tidal period T is such that $w/UT < 0.13$, we find that dipoles can propagate away from the source region without being drawn back into the sink. Some results of this process are also presented from a depth-averaged numerical model of a realistic oceanographic situation.

1 Introduction

Separation of tidal flow past a sharp headland can lead to the formation of a recirculating eddy. When the strength of vorticity associated with these eddies is weak and bottom dissipation strong, their effect on the mixing and dispersion of passive tracers, can be well described by averaging over many tidal periods and so determining a “residual flow field” (Zimmerman, 1986). However, when the length of tidal excursion becomes larger than the scale of the headlands, the strong time dependence of the flow field implies that averaging can lead to misleading impressions of the mixing. If vortices are long-lived they will change the mixing properties of the tidal flow, as the circulation in a vortex leads to a barrier to transport across its perimeter (Provenzale, 1999). Such transport of sediment within the cores of coherent tidal vortices has been implicated in the formation of sand banks near headlands (Pingree, 1978, Pingree & Maddock, 1979).

The role of eddies must be explicitly considered in tidal flows if multiple eddies are present and can interact. This situation can arise if eddies survive multiple tidal cycles or if eddies form at multiple headlands that are separated by less than the tidal excursion. An example of this is discussed by Pawlak & McCready (2002) where the residual currents formed by eddy

formation at a headland can change direction from on-shore to off-shore, if eddy lifetimes increase beyond a tidal period. Another case of such vortex interaction is for tidal flow through a narrow channel between a basin and the sea. Here vorticity formed in the channel can lead to the formation of two large counter-rotating vortices. If these structures are sufficiently long-lived they can form a coherent dipole structure that can self-propagate away from the channel. Observations in the semi-enclosed Seto Sea in Japan (Fujiwara et al., 1994), have revealed that on the flood tide, long-lived self-propagating dipoles can form that lead to a strong flushing mechanism between basins. These dipole structures were also crucial in determining the mean circulation in the Kyoto bay and had an important role in sediment transport and bank formation. This has been previously studied theoretically and experimentally by Kashiwai (1984, 1985), who found that such tidal dipoles could propagate away from the channel if a dimensionless ratio w/UT (where U is the maximum velocity, w the width of channel and T the tidal period) was less than 0.09. Similar types of dipole structures have been observed in numerical simulations of the flushing of confined harbours and estuaries (Signell & Butman, 1992, Brown et al., 2001).

The important effect of such dipole formation is

that there will be greatly enhanced flushing between the basin and sea, compared to the classical idea of tidal pumping by the source-sink asymmetry (Stommel & Farmer, 1952). In this conceptual picture, flow separation leads to an asymmetry between the flow in and out of the channel so that a fraction of water that escapes as the jet is not sucked in by the sink flow. If flow out of the channel forms a dipole then it may have a large enough self-propagation velocity that it moves away from the channel and is not sucked back on the returning tide. In this case almost none of the water that leaves the channel will return on the next tide.

In this paper we discuss a theoretical and laboratory model of the formation of dipoles in an oscillating flow through a narrow channel connecting two basins. Particular attention is focused on the conditions necessary for a dipole formed during the out-flowing period, to escape from the influence of a returning sink flow. In §2 we introduce a simple theoretical model of the dipole and sink properties, and determine the critical value of the ratio w/UT , necessary for a dipole to escape from the channel. Our resulting critical value is slightly higher than that of Kashiwai (1974) due to our different assumptions. In §3 we discuss observations of dipole formation in laboratory experiments as a function of w/UT . The implication of our laminar laboratory experiments to the case of the turbulent ocean is discussed in §5, where we present results from a numerical simulation of tidal flow in a realistic oceanographic setting, and look at the additional effects of changing the channel profile, maximum depth and drag co-efficient.

2 Theory

The asymmetry between the inflow and outflow is sketched in figures 1 and 2. When fluid flows out of the channel, the no-slip condition leads to the growth of viscous boundary layers, which contain large amplitude vorticity. At the sharp corner, the flow separates and the detached sheet of strong vorticity rolls up on itself to create a vortex. Two such vortices are created at the opposite sides of the channel mouth, which may couple together and form a dipole. This is a coherent structure which will propagate with a speed proportional to the total amount of vorticity in each vortex, and inversely proportional to their separation distance. On the other hand, flow into the channel will resemble a potential sink flow, where the magnitude of velocity decreases inversely with distance from the channel mouth. In an oscillating tidal flow through a channel, a dipole formed on one phase of the tide may escape the sink flow if the dipole propagation velocity is greater than the local velocity due to the sink flow.

In the following subsections we will introduce a

simple model of the trajectory of the dipole. The dipole is treated as consisting of two point vortices, whose circulation is a function of time and related to the velocity in the channel. The flow into the channel is treated as a potential sink flow. By numerically integrating the resulting analytic expressions we obtain dipole trajectories and can determine if a dipole is able to escape from the channel mouth after a tidal period as a function of the width of the channel w , the maximum channel velocity U , and the tidal period T .

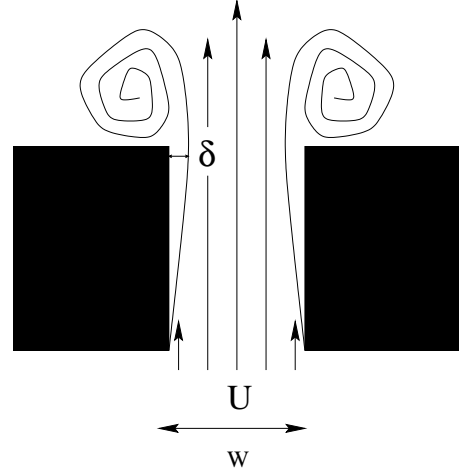


Figure 1: Flow leaving a sharp channel may induce formation of a dipole, by advection of vorticity created at the boundaries.

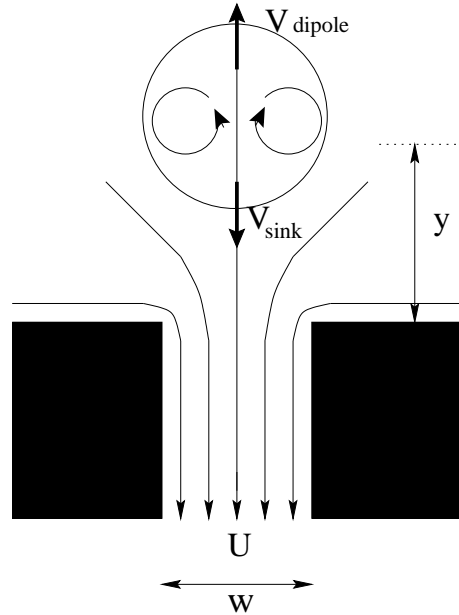


Figure 2: Flow returning into the channel can be described by a potential sink. As vortex structures can be long-lived, the situation at ebb tide may now involve a self-propagating dipole and sink flow.

2.1 Properties of the dipole

A simple model for the formation process of a dipole is to consider the total injection of vorticity created at

no-slip walls (Shariff & Leonard 1992). In this “slug” model there is a constant velocity U acting for a time t . A viscous boundary layer forms at the wall that has a thickness δ . Within this layer the average vorticity will scale as $\omega = U/\delta$ and the average velocity will scale as $U/2$. As the circulation is the area integral of the vorticity, the total vorticity advected from the nozzle at time t can be estimated as

$$\Gamma = \int \int_A \underline{\omega} \cdot \underline{n} dA \sim \frac{U}{\delta} \times \delta \times U/2 \times t = \frac{1}{2}U^2t \quad (1)$$

This can also be written as $\Gamma = 1/2 UL$ where L is the length of the slug. This scaling argument has fairly good agreement with experimental observations when the ratio slug length L to width w is greater than 1.5. For $L/w < 0.5$, however the predicted circulation is systematically lower than experimental observations of vortex rings by about 50 % (Shariff & Leonard 1992). We expect similar results to hold for quasi 2D dipoles.

In depth-averaged models of shallow water flow vorticity is usually generated by the effect of increasing drag in shallow waters, so that the width of the strong vorticity is much greater than predicted by a horizontal eddy diffusivity. However the circulation is an integral of the total vorticity so that (1) should still be valid for these cases.

Two vortices of opposite signs are able to induce a movement in each other so that a self-propagating dipole structure can emerge. A simple model of this dipole, is to consider two point vortices of strength $\pm\Gamma$; the translation velocity induced by these two point vortices is then

$$V_{dipole} = \frac{\Gamma}{2\pi a} \quad (2)$$

with a the distance between the point vortices.

2.2 Properties of the sink flow

A small distance ($y \gg w$) away from the channel, the sink flow velocity field will resemble that of a potential sink, whereby the velocity decreases inversely with distance so that along the y axis

$$V_{sink} = \frac{Uw}{4\pi y} \quad (3)$$

2.3 Competition between the dipole and the sink

To understand how a dipole may escape from an oscillating flow in a channel we first consider the simple case where the velocity in the channel changes abruptly from a source to a sink, like a square wave. If a dipole is produced on one phase of this flow, there is the possibility that the self-advection velocity (2) will be greater than the velocity of the sink (3). Using (1)

to scale Γ we find that the propagation velocity of the dipole is greater than the velocity when

$$\frac{Y}{w} > \frac{2a}{UT}, \quad (4)$$

with Y the y co-ordinate of the dipole position. Thus there is a critical distance Y that a dipole must pass before it can escape the effect of subsequent return flow. The question then becomes a matter of determining where the centre of the dipole is on the y -axis. If Γ increases linearly with time as $\Gamma = 1/2U^2t$ then the dipole velocity is also a function of time. The total distance the dipole moves in the period $T/2$ is then

$$Y = \int_0^{T/2} \frac{U^2t}{4\pi a} dt \implies Y_o = \frac{U^2T^2}{32\pi a}. \quad (5)$$

Substituting (5) into (4), tells us that the critical distance will be exceeded when

$$\frac{a}{UT} < (64\pi/c)^{-1/3} \quad (6)$$

where $c = a/w$. Experimental results for this case (Wells & van Heijst, 2003) found that the ratio of the dipole separation a to the width w is typically in the range $1 < a/w < 1.5$. In this case the critical value is then in the range 0.171 to 0.130. In the following discussion of a sinusoidal flow we will only consider $c = 1$.

2.4 Dipole trajectories for a sinusoidal forcing

We predict the trajectory of the dipole using a similar analysis to Kashiwai (1974). For the case of a sinusoidal forcing with time dependent velocity $U(t) = U_o \sin(2\pi t/T)$, the circulation of the two vortices will be expressed as $\Gamma = 1/2 \int U(t)^2 dt$ by (1). We assume that the circulation of the dipole is produced vorticity is produced on the flood tide, and then remains constant. The dipole moves by integration of (2) for $t < T/2$, and for $t > T/2$ there is the additional influence of the sink flow described by (3). Then we can write equations of motion for the center of the dipole as

$$\frac{\partial Y}{\partial t} = \begin{cases} \frac{U^2t}{4\pi d} \left(t - \frac{\sin(4\pi t/T)}{4\pi/T} \right) & 0 < t < T/2 \\ \frac{U^2T}{16\pi d} - \frac{Ua \sin(2\pi t/T)}{4\pi y} & T/2 < t < T \end{cases} \quad (7)$$

Integrating the dipole excursion using (5), with a sinusoidal velocity results in $Y_o = U_o^2T^2/64\pi a$, a factor of 2 lower than for the square wave. The equations (7) are non-dimensionalized by the period T and the distance Y_o to give

$$\frac{\partial Y^*}{\partial t^*} = \begin{cases} 8 \left(t^* - \frac{\sin(4\pi t^*)}{4\pi} \right) & 0 < t^* < 1/2 \\ 4 - \left(\frac{a}{UT} \right)^3 \frac{1024 \pi \sin(2\pi t^*)}{c Y^*} & 1/2 < t^* < 1 \end{cases} \quad (8)$$

This is plotted in figure 3 for different values of w/UT . As the sink velocity is now a function of time no steady solution is possible, as was the case for a square wave. It appears that for $w/UT > 0.1296$ the dipole will be sucked back into the sink and for $w/UT < 0.1229$ it can escape. This value is higher than Kashiawi (1974), who predicted a critical value of 0.94. This difference is due to the factor of 1/2 we use in Eq. (1), rather than the incorrect value of 1; and due to the assumption of Kashiawi that the dipole remains stationary for $0 < t < T/4$.

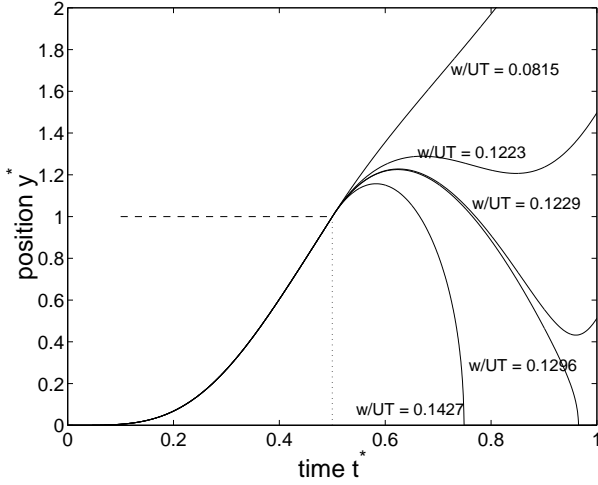


Figure 3: Dipole position $Y^*(t^*)$ for different values of w/UT , with a channel velocity varying sinusoidally in time. This figure was obtained from integration of (8).

3 Experimental design

To simulate tidal flow through a narrow channel, and observe the behaviour of dipole formation, a detailed series of experiments were conducted. The most important consideration in these experiments was to make the flow quasi-two dimensional and laminar, so that the analysis from §2.4 is relevant.

The experiment is sketched in figure 4 and consisted of a tank of dimensions $500\text{mm} \times 1500\text{mm} \times 300\text{mm}$, divided into two “basins” by a Plexiglas wall. Fluid flows from one basin to the other through a small channel, whose width can be varied. To drive the flow a cylinder of cross-sectional area $A = 1960\text{mm}^2$ is slowly lifted up and down by a cable connected to a rotating disk. To maintain constant water level, fluid must flow between the two basins. The velocity and period of this “tidal” flow are controlled by changing either the amplitude Δh , the period T of the oscillating cylinder or the cross-sectional area of the channel. We can estimate the maximum velocity by assuming that all the water displaced by the cylinder flows through the channel. This is a reasonable assumption if the period of the cylinder oscillation is much longer than the time a wave takes to propagate

through the basins, and that the frequency of oscillation is far from a resonant frequency of the system. To study the behavior of dipoles as a function of the ratio w/UT we vary the width w and depth of fluid d while keeping the period T and amplitude Δh constant at $T = 10\text{ s}$ and $\Delta h = 12\text{ mm}$.

In order to make the flow quasi two-dimensional we found that the addition of a very thin ($\sim 1 - 2\text{ mm}$) layer of dense salty water, appeared to substantially delay the onset of three-dimensional instabilities of the vortices.

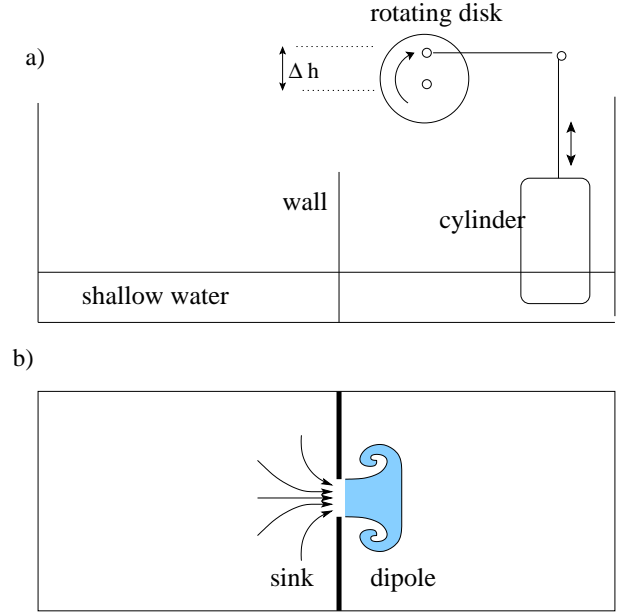


Figure 4: The experimental set-up, where a sinusoidal flow was forced by means of a cylinder oscillating up and down. This can be seen in the side view of (a), where a cable is connected from the cylinder to a rotating disk. The resulting flow pattern is sketched as seen from above in (b), where the water is moving from the left to the right. This flow has the form of a sink on the left-hand side and the form of a dipole on the right-hand side.

4 Laboratory results

Photographs of two different types of flow evolution are shown in figures 5 and 6. The first set of photos were taken using an apparatus capable of square wave forcing (Wells & Van Heijst, 2003) and a dipole can be clearly seen; the subsequent image is taken one period later and shows another dipole which also propagates collinearly with the first. The second series of photographs in figure 6 are taken using the apparatus sketched in figure 4 and show the case where a dipole forms, but then a large proportion is sucked back into the channel when the flow changes direction.

The two sequences of photographs show clearly defined examples of where dipoles either escape or get sucked back into the channel. Near the critical

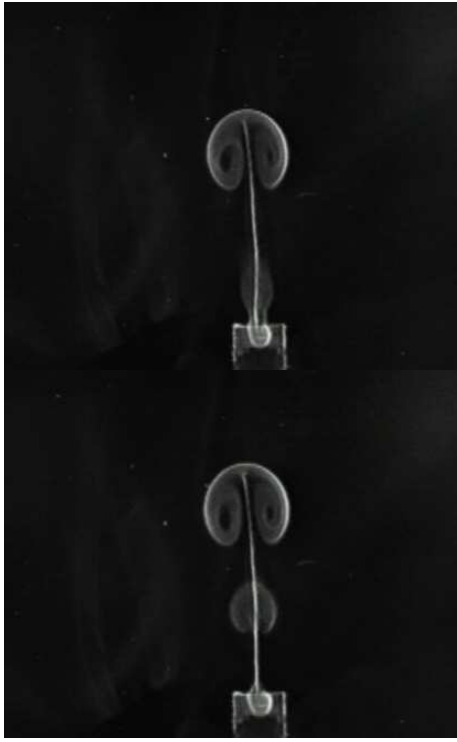


Figure 5: Laboratory visualization of the dipoles propagating away from a channel, from an experiment capable of square wave forcing (Wells & van Heijst, 2003). The nozzle has a width of 50 mm and here $w/UT = 0.05$. The photographs were taken one forcing period apart.

value of w/UT the differences in regimes are not clearly observed, as part of the dipole appears to be stripped off, while part escapes. However, for most experiments we were able to distinguish the two different regimes and the resulting classifications have been marked in figures 7. The observations show good agreement with the theory, despite a little scatter near the critical value of $w/UT = 0.13$. We note that these results are also consistent with the 5 experiments of Kashiwai (1974) who found the same transition to occur between the two of his experiments that had values of $w/UT = 0.085$ and 0.182 .

5 Generation of vortices in oceanographic situations.

In our laboratory experiments the flow is laminar and three-dimensional effects are relatively small, unlike typical tidal flows in the ocean. However, many of the ideas developed in this paper are expected to still apply to tidal flushing in estuaries, harbours and fjords when sufficiently large scales are studied where the ideas of “eddy diffusivity” are applicable. Formation of transient eddies by tidal flows has recently been studied by many authors (see e.g. Awaji, et al. 1980, Signell & Geyer 1991) using various forms of depth-averaged equations. In such models, the creation of vorticity is no-longer primarily due to no-slip boundaries but rather the way that stress is parameterized. In

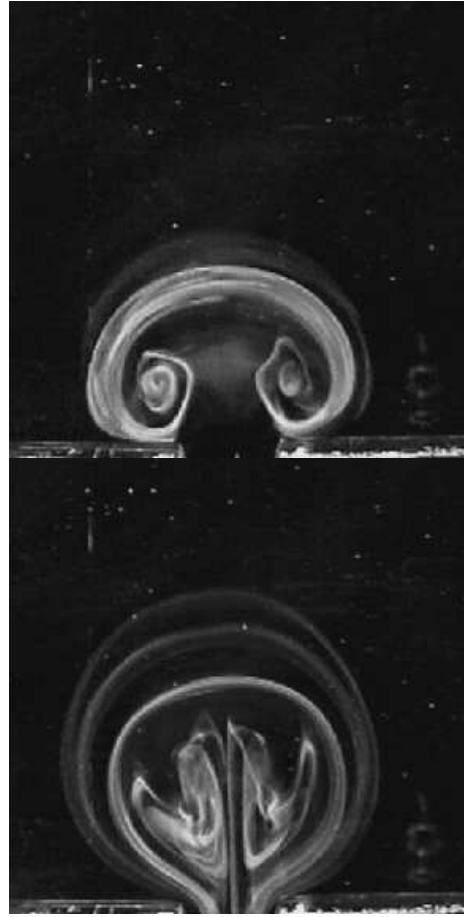


Figure 6: Laboratory visualization of a dipole being sucked back through the channel. The nozzle has a width of 30 mm, maximum velocities were $U = 12\text{mm s}^{-1}$ and $T = 12\text{s}$ so that and here $w/UT = 0.21$. The photographs are taken at (a) 4 s and (b) 10 s during the 12 s cycle.

many numerical models the bed stress due to 3D turbulence is parameterized with an inverse dependence upon depth, using a quadratic drag law of the form

$$\tau_b = \rho C_D |\mathbf{U}| \mathbf{U} \quad (9)$$

with a drag coefficient of $C_D = 2.5 \times 10^{-3}$ being typically used in civil engineering practice, see e.g. Fischer (1979). At horizontal boundaries where the depth goes to zero, the flow velocity contains a gradient, with zero velocity at the edge. This condition implies generation of vorticity. While bed stress acts as a mechanism to create vorticity in regions of strong bathymetry, it can also leads to decay of vorticity. A horizontal eddy diffusivity is also used in most numerical models to model horizontal diffusion of momentum by the effects of unresolved 3D turbulence. This eddy diffusivity can also create vorticity, but only very near boundaries.

The momentum equation of such shallow water flows is given by

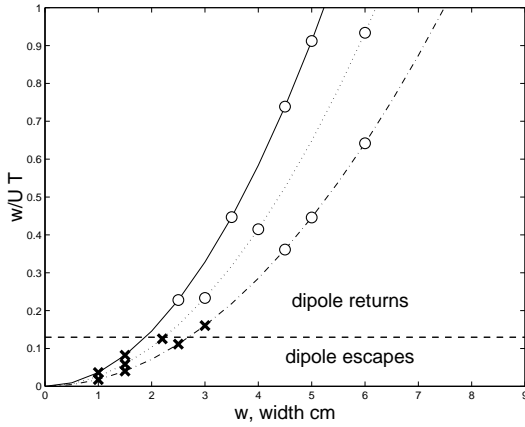


Figure 7: Experimental results using the apparatus sketched in figure 7. A cross (\times) indicates experiments where the dipole can escape and a circle (\circ) indicates those where the dipole returns to the sink. To vary the ratio w/UT the width of the channel was varied for a particular depth d . The three different depths used were $d = 20$ mm — —, $d = 30$ mm \cdots and $d = 40$ mm — \cdot —. The horizontal broken line represents for the critical value of $w/UT = 0.13$

$$\frac{\partial \mathbf{U}}{\partial t} + \mathbf{U} \cdot \nabla \mathbf{U} = -g \frac{\partial \eta}{\partial t} - \frac{C_D |\mathbf{U}| \mathbf{U}}{h} + A_h \frac{\partial^2 \mathbf{U}}{\partial x^2} \quad (10)$$

where η is the elevation of the free surface.

There are two timescales in (10) associated with the decay of velocity: the first due to the quadratic drag term,

$$t_{drag} = \frac{h}{C_D U} \quad (11)$$

and the second due to horizontal diffusion of

$$t_{diff} = \frac{L^2}{A_h} \quad (12)$$

where L is the width of the eddy and A_h a horizontal eddy diffusivity of momentum. The first time scale is related to the decay of vorticity and circulation by bottom drag processes, whereas the second time scale is related to the horizontal diffusion of vorticity. Away from horizontal boundaries this will lead to a decay in velocities and hence peak vorticity, but not of the circulation. Thus in terms of calculating the vortex trajectory (which depends upon the circulation Γ), the timescale t_{drag} is most important. This lead Signell & Geyer (1991) to introduce a length-scale of $L = U t_{drag}$ over which the expected vorticity to decay. This length-scale has a linear dependence on water depth, so that for greater depths dipoles may propagate over larger distances. In their simulations using $C_D = 2.5 \times 10^{-3}$ and tidal velocities of about 1 m s^{-1} , Signell & Geyer (1991) found that eddies formed in water deeper than about 40 m, would survive longer

than half a tidal period. As their simulations can be viewed as one half of our channel, this gives a good indication of when we might expect our process to be important.

The process of tidal flushing in a more realistic oceanographic setting was studied by making a numerical simulation of an idealized tidal basin using the DELFT-3D code. An example of a bathymetry used in the calculations is sketched in figure 8. The laboratory experiments discussed earlier placed emphasis on the maximum velocity in the channel, width of channel and tidal period. There are at least three additional parameters that are important for a depth-averaged simulation of a realistic tidal channel, namely the shape of the channel profile, the maximum depth and how bottom drag is parameterized. The simulation shown in figure 9 is interesting in that a dipole is seen to form, but it does not propagate away from the channel, even though the measured ratio w/UT exceeds the critical value. It appears that this is due to the rapid decay of peak velocities in the vortices by bottom drag when the maximum depth is 20 m and $C_D = 2.5 \times 10^{-3}$. If we keep the same channel width and forcing but change either the maximum depth to 40m or reduce drag co-efficient by half to $C_D = 1.25 \times 10^{-3}$, then dipoles are able to propagate further away from the channel. Despite a dipole clearly forming in figure 9, there is rather weak flushing as the dipole decays rapidly. The effect of the changing the channel profile has an important impact on the width of the vortex strip that is produced. As opposed to laboratory experiments where the width of the boundary layer is set by horizontal diffusion of momentum, in these shallow water flows the width is largely set by the underlying bathymetry. This results in much wider vortex strips than would be predicted using a horizontal eddy diffusivity. For the same maximum velocity in the channel, the total amount of vorticity produced should be the same but it will be spread over a wider region and so will change the large scale mixing dynamics. This can be clearly seen in figure 9, where vorticity is produced over the full width of the channel. For a modeling view point it is then essential to have sufficiently high resolution of the bathymetry at shallow boundaries in order to capture the generation of vortices accurately. The neglect of this process may lead to underestimating the mixing and transport of pollutants and sediments in these regions.

5.1 Flushing in oceanographic observations and other numerical simulations

Oceanographic observations of this process were seen in the Naruto Strait, where strong dipoles are formed and propagate away from the channel. In this case the maximum velocity was about 4.5 m s^{-1} and the max-

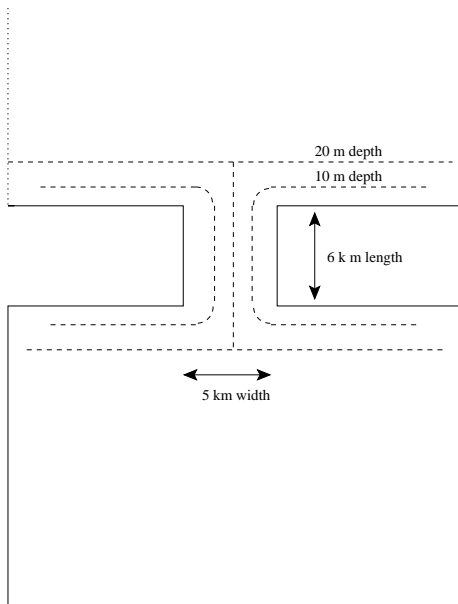


Figure 8: The bathymetry used in numerical simulations. The channel width was 5 km with a maximum depth of 20 m, the length of the channel was 6 km. The flow was forced by setting the tidal amplitude at the boundaries of the top basin to 1 m. The bottom basin had solid boundaries. A resolution of $100\text{ m} \times 100\text{ m}$ was used, so that the sloping boundaries are well resolved.

imum depths of $H \sim 100\text{ m}$ (Awaji, 1980). A similar observation was made in the flushing of the Venice lagoon, where maximum $U \sim 1\text{ m s}^{-1}$ and $H \sim 20\text{ m}$ (Gacic et al. 2002). In geometrically similar channels of the Wadden Sea where U is about 1 m s^{-1} and the maximum water depths are around 10 m, bottom dissipation was strong enough to prevent any strong vortices from forming (Ridderinkhof, 1990). Images in a numerical simulation of tidal flushing of Boston Harbour by Signell & Butman (1992) show an indication of a propagating dipole (where $U \sim 0.5\text{ m s}^{-1}$ and $H \sim 20\text{ m}$), but a similar dipole formed in a related simulation of flushing of a tidal estuary in the Gulf of Texas (Brown et al. 2001) where $U \sim 0.5 - 1\text{ m s}^{-1}$ and $H \sim 15\text{ m}$, does not propagate away. In both cases the flow exceeds the criterion of $w/UT < 0.13$, so we assume the difference is due to differences in parameterization of bottom dissipation. It would be useful in future simulations to see how sensitive vortex generation and the subsequent mixing are to differences in the value of the bottom drag coefficient.

5.2 Other flushing processes

In addition to the mechanism of dipole flushing discussed in this paper, there are also many other processes that may be more important in a particular oceanographic situation, for determining the exchange of water between a semi-enclosed basin and the ocean. In estuaries, strong stratification can arise

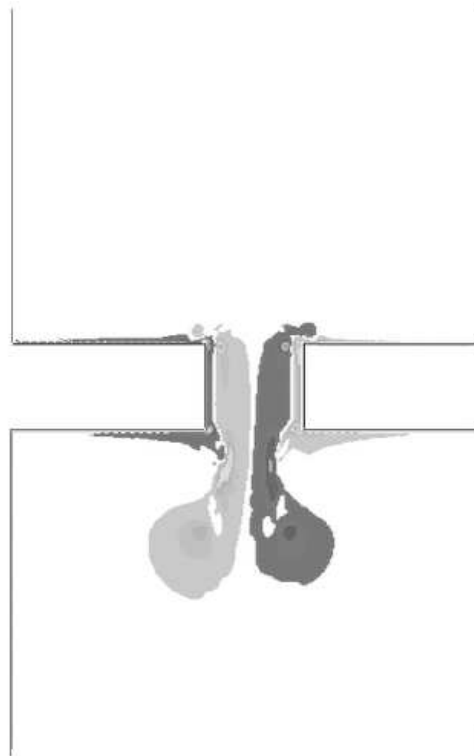


Figure 9: The vorticity produced by flow through a 5 km wide channel, from a simulation using the DELFT-3D code. The dark/light gray represents positive/negative vorticity with peak values of $\pm 0.1\text{ s}^{-1}$ and mean values of $\pm 0.05\text{ s}^{-1}$, respectively. Maximum velocities were 1 m s^{-1} but due to the shallow depth of the water (20m), the dipoles decay rapidly and do not propagate away from the channel mouth, even though $w/UT \ll 0.13$ for this experiment.

due to fresh inflow from a river, or from surface evaporation, so that a two-layer exchange flow can be the rate-limiting mechanism in flushing an estuary. Such a flow with the addition of tides leads to complicated vortex patterns (Kapolnai et al. 1996), which are different from the present study. Most real channels will be asymmetric, which will probably lead to increases in the exchange rates. Hydraulic models of Kashiwai (1985), using a variety of asymmetric channels, found that asymmetric dipoles would form, leading to curved trajectories and greater flushing than considered here. Even in symmetric channels, the inclusion of the Coriolis forces will lead to an asymmetry in the jet leaving the channel. Along-shore coastal currents will likely make a very large change from our idealized picture. These can be the result of large-scale circulations (like the Gulf Stream), responses to short term fluctuations such as wind forcing or due to the tidal forcing itself. There are of course, many regions of the ocean that do not experience strong variation in tides along the coast and it is these settings that our model may be applicable to. Such small variations in tidal phases were reported for the region surround-

ing Boston by Signell & Butman (1992), so that in their numerical model of the tidal flushing of Boston Harbour, structures emerged that looked similar to the dipoles which are reported in this paper.

6 Conclusion

Our experiments have shown that dipoles can form when a tidal flow passes through a channel, and that these dipoles may propagate away from the channel region. This leads to an increase in the exchange between two basins compared to the model of Stommel & Farmer (1952). Such a process may be an important mechanism of exchange and transport of water bodies, and the associated chemicals and sediment within them. As such it is crucial for a numerical model used for coastal oceanography applications, to accurately model the bathymetry close to coast-lines, as these shallow and sloping regions are where most vorticity is generated and dissipated. The effect of dipole formation on flushing reported in this paper, and related currents associated with vortex generation around multiple headlands studied by Pawlak & McCready (2002), show that if flow separation and vortex generation is neglected the magnitudes of mixing rates may be largely underestimated. As the decay of circulation in such vortices is largely controlled by bottom drag in oceanographic settings, these effects will be most important in deep waters (>30m depth), where vortices can persist for longer than a tidal cycle.

7 Acknowledgments

We would like to thank Rob Uittenbogaard (Delft Hydraulics) for use of the DELFT-3D code, and for many useful discussions.

8 References

Awaji, T.A., Imasato, N. & Kunishi, H. (1980) Tidal exchange through a strait: A numerical experiment using a simple model basin. *J. Phys. Oceanogr.* **10**, 1499-1508.

Awaji, T.A. (1980) Tidal Exchange through Naruto, Akashi and Kitan Straits *J. Ocean. Soc. Japan* **36**, 151-162.

Brown, C.A., Jackson, G.A. & Brooks, D.A. (2001) Particle transport through a narrow tidal inlet due to tidal forcing and implications for larval transport. *J. Geophys. Res.* **105**, 24,141-24,156.

Fischer, H.B. (1979) *Mixing in Inland and Coastal Waters*. Academic Press, New York.

Fujiwara, T., Nakata, H. & Nakatsuji, K. (1994) Tidal-jet and vortex-pair driving of the residual circulation in a tidal estuary. *Cont. Shelf Res.* **14**, 1025-1038.

Gacic, M., Kovacevic, V., Mazzoldi, A., Paduan, J., Arena, F., Mancero Mosquera, I., Gelsi, G. & Ar-

cari, G. (2002) Measuring water exchange between the Venetian Lagoon and the open sea. *EOS Trans. AGU.* **83(20)**, 217-222.

Geyer, W.R., & Signell, R. (1990) Measurements of tidal flow around a Headland with a shipboard acoustic Doppler current profiler. *J. Geophys. Res.* **95**, 3189-3197.

Kashiwai, M. (1984) Tidal residual circulation produced by a tidal vortex, Part 1 Life history of a tidal vortex. *J. Ocean. Soc. Japan* **40**, 279-294.

Kashiwai, M. (1985) TIDICS - Control of tidal residual circulation and tidal exchange in a channel-basin system. *J. Ocean. Soc. Japan* **41**, 1-10.

Kapolnai, A., Werner, F.E. & Blanton, J.O. (1996) Circulation, mixing, and exchange processes in the vicinity of tidal inlets: A numerical study *J. Geophys. Res.* **101**, 14,253-14,268.

Pawlak, G. & MacCready, P. (2002) Oscillatory flow across an irregular boundary. *J. Geophys. Res.* **107**, 3-1 3-17.

Pingree, R.D. (1978) The formation of the Shambles and other banks by tidal stirring of the seas. *J. Mar. Bio. Ass. U.K.* **58**, 211-226.

Pingree, R.D. & Maddock, L. (1979) The tidal physics of headland flows and offshore tidal bank formation. *Marine Geology* **32**, 269-289.

Provenzale, A. (1999) Transport by coherent barotropic vortices. *Ann. Rev. Fluid Mech.* **31**, 55-93.

Ridderinkhof, H. (1990) *Residual currents and mixing in the Wadden Sea*. PhD thesis. Utrecht University, the Netherlands.

Shariff, K. & Leonard, A. (1992) Vortex rings. *Ann. Rev. Fluid Mech.* **24**, 235-279.

Signell, R.P. & Geyer, W.R. (1991) Transient eddy formation around headlands. *J. Geophys. Res.* **96**, 2561-2575.

Signell, R.P. & Butman, B. (1992) Modeling tidal exchange and dispersion in Boston harbour. *J. Geophys. Res.* **97**, 15,591-16,606.

Stommel, H. & Farmer, H.G. (1952) On the nature estuarine circulation. *WHOI Tech. Rep.* **52-88**, pp. 131.

Wells, M.G. & van Heijst, G.J.F. (2003) A model of tidal flushing of an estuary due to periodic dipole formation. *Dyn. Atmos. Oceans* (submitted).

Zimmerman, J.T.F. (1986) The tidal whirlpool; A review of horizontal dispersion by tidal and residual current. *Neth. J. Sea Res.* **20**, 133-154.